NCREE Special Newsletter

Summary of the Hualien Earthquake Event on April 3, 2024

1. Overview of Earthquake and Disaster Survey

On April 3, 2024, at 7:58 a.m., a Richter scale 7.2 earthquake occurred offshore Hualien, with its epicenter at approximately 23.77° north latitude and 121.66° east longitude, with a depth of 15.5 km, as reported by the Central Weather Bureau (Figure 1-1). This seismic event registered intensity 6 strong and 6 weak in Heping Township and Hualien City, Hualien County, resulting in significant damage to buildings and incidents of rockfall. Following the consolidation of relevant damage information by the Central Weather Bureau on April 3, the National Seismological Center promptly dispatched personnel to conduct damage assessments in Hualien and the surrounding areas. The on-site reconnaissance operations encompassed surveys of residential structures, school buildings, medical facilities, and non-building structures for damage assessment.

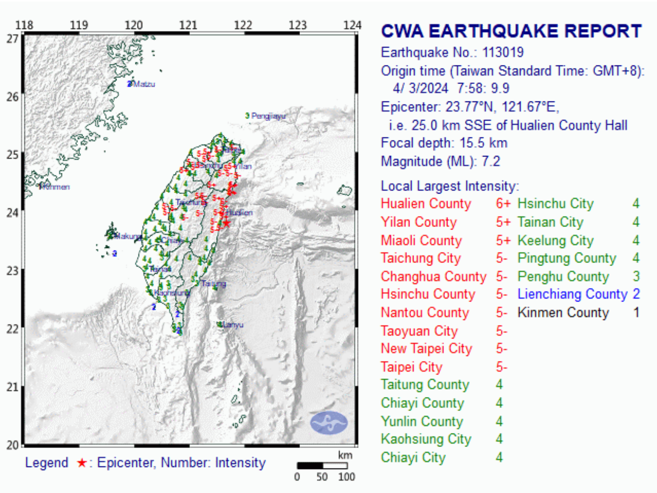

Figure 1-1 Central Weather Bureau's Report on the Richter Scale ML7.2 Earthquake on April 3rd

2 - Evaluation of the Seismic Source and Strong Ground Motions

The ML 7.2 (moment magnitude MW 7.4) Hualien earthquake exhibited a reverse-fault mechanism associated with a few strike-slip components, and the focal depth was 15.5 km, according to rapid location reports by Taiwan's Central Weather Administration (CWA). The moment tensor solutions obtained by the United States Geological Survey (USGS), Incorporated Research Institutions for Seismology (IRIS), and the Global Real-Time Moment Tensor Monitoring System by IES (GRMT) exhibit similar features, as shown in Fig. 2-1.

The CWA reported 1,416 aftershock events occurring up to one month later (May 9) (Fig. 2-2), including four events with magnitudes greater than 6, with the highest intensity being 5+.

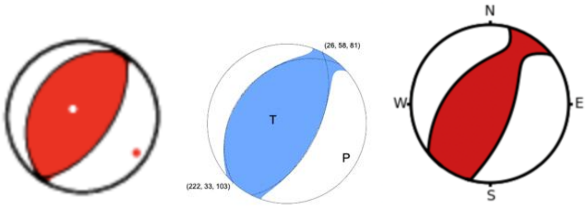

Fig. 2-1 Focal mechanisms for this event from GRMT, USGS, and IRIS from left to right.

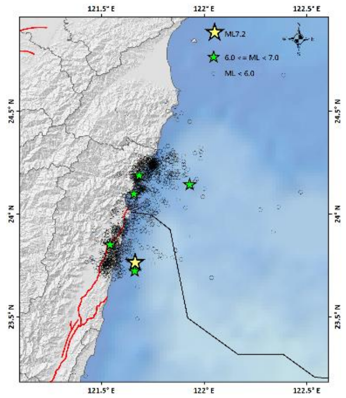

Fig. 2-2 Distribution map of the aftershock sequences until May 9 reported by the CWA of Taiwan.

The largest peak ground acceleration (PGA) and peak ground velocity (PGV) recordings observed at Station EHP (和平) were approximately 363.7 gal and 65.7 cm/s, respectively, based on seismic networks operated by the CWA. In Hualien County, the PGA and PGV were approximately 458 gal and 57.7 cm/s at Station HWA (花蓮市). Fig. 2-3 shows the three components of the acceleration time series recorded at stations EHP and HWA. Fig. 2-4 shows ground-motion shake maps, including real-time observations and Taiwan's new ground-motion model, which was developed using observed ground motions (Chao et al., 2020). These shake maps provide ground-motion information, including PGA and PGV, as well as spectral acceleration at 0.3 s (Sa0.3) and 1 s (Sa1.0), which assist in evaluating the correlation between strong ground motions, their causes, and building responses. The PGA shake map is a reference that indicates the approximate PGA values for comparison with damage to buildings due to the earthquake. High seismic shaking (Fig. 2-5) is observed, with the main high-intensity areas of the earthquake concentrated in the Hualien region and the southern part of Yilan.

Fig. 2-5 compares the design spectra (by Taiwan building code in 111 version) with the observed response spectra of the EHP and HWA stations, which recorded the highest intensities (6+ and 6- on the CWA-defined scale) and the highest spectral acceleration in a 1-second oscillator period. From the observed response spectra, it is evident that these two stations exhibit high spectral acceleration values in considerably short periods, but the values for the medium- to long-oscillator periods are lower than the design spectra. The maximum spectral accelerations observed at these two stations are close to the Maximum Considered Earthquake (MCE) at approximately 1 second oscillator period. Comparing the response spectra reveals that spectral accelerations exceed the design spectra at a few oscillator periods, indicating that buildings may experience slight damage if their predominant periods align closely with these resonant periods.

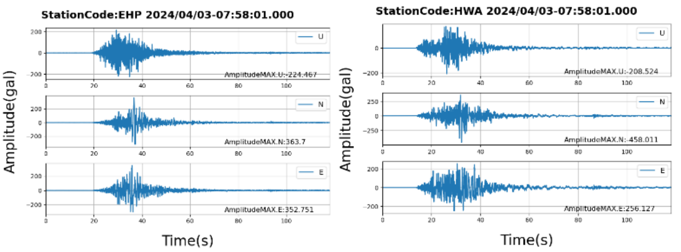

Fig. 2-3 Three components of the acceleration time series recorded at the EHP and HWA stations. Upper panel: vertical direction; middle panel: NS horizontal direction; lower panel: EW horizontal direction.

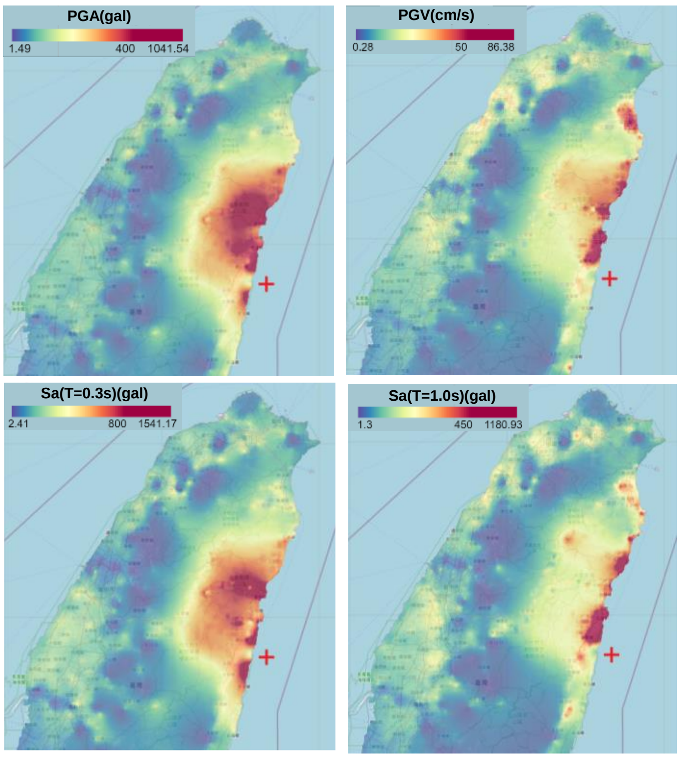

Fig. 2-4 Shake maps from the real-time NCREE platform for ground-motion information, which gathered data from several seismic observation networks, including CWBSN, TSMIP, SANTA, and EEWS. Upper left: peak ground acceleration (PGA); upper right: peak ground velocity (PGV); lower left: spectral acceleration at 0.3 s (Sa0.3); and lower right: spectral acceleration at 1.0 s (Sa1.0).

.

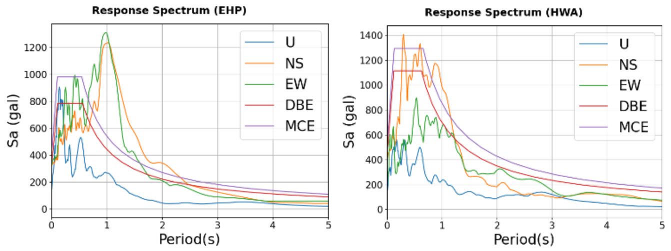

Fig. 2-5 Comparison of the observed response spectrum and the design response spectrum of two stations: the EHP station with the largest seismic intensity (left) and the HWA station with the maximum 1-second period spectral acceleration (right).

3. TELES Earthquake Damage Estimation

The focal mechanism solutions provided by both the USGS and GRMT indicate a similar seismic source mechanism, characterized by a reverse faulting rupture style, with the rupture direction and dip angle being roughly consistent. Considering the current inability to confirm the actual orientation of the fault rupture surface, two potential fault rupture surface scenarios are considered separately for seismic event modeling. The Taiwan Earthquake Loss Estimation System (TELES) is then employed to assess seismic damage in accordance with these scenarios.

We refer to the USGS mechanism solution to set the orientation and dip angle of the fault rupture plane. Scenario 1 assumes a fault rupture surface oriented approximately northwestward, similar to the orientation of the subduction zone system in the region. It is hypothesized that Scenario 1 represents an earthquake caused by a subduction zone interface rupture. The length and width of the rupture surface are estimated using empirical equations applicable to subduction zone interface ruptures, and seismic ground motion is estimated using a prediction model suitable for this type of seismic source. Scenario 2 assumes a fault rupture surface oriented roughly southeastward, representing an earthquake caused by a reverse fault. Empirical equations relevant to reverse faults are applied to estimate the length and width of the rupture surface, and seismic ground motion is estimated using a prediction model specific to reverse faults. For detailed information on the fault rupture surface locations, specific source parameters, and TELES intensity distribution estimates for both scenarios, please refer to Figure 3-1.

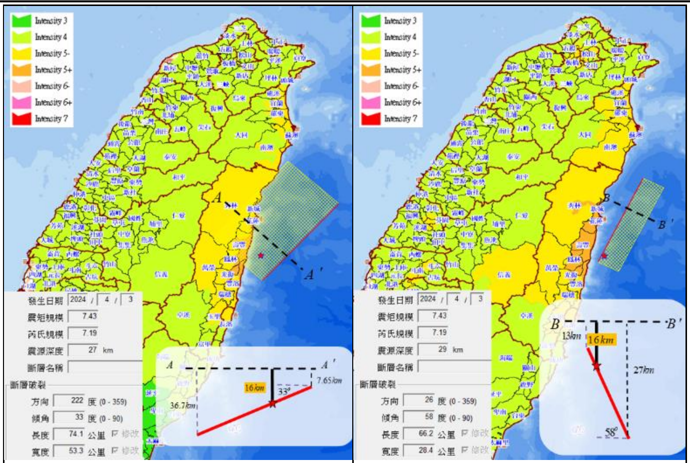

Scenario 1: Northwestward inclination, subduction zone interface seismic source

Scenario 2: Southeastward inclination, reverse fault

Figure 3-1 TELES Earthquake Damage Assessment Scenarios

Based on the aforementioned seismic scenarios, the estimated building damage and casualties using TELES are presented in Tables 3-1 to 3-4. For Scenario 1, the assessment results indicate a total of 78 buildings collapsed or partially collapsed, resulting in 7 fatalities and severe injuries due to building damage. In Scenario 2, the assessment results show a total of 650 buildings collapsed or partially collapsed, leading to 104 fatalities and severe injuries due to building damage. The most severely affected area in both scenarios is Hualien City.

The actual impact of the earthquake resulted in 18 fatalities, 1,155 injuries, 37 individuals displaced, and 2 persons missing (as of April 25); casualties were primarily attributed to slope-related disasters such as landslides and rockfalls. Notable building damages include the collapse and tilting of the Uranus Building (1 fatality, 4 injuries) and the tilting of the Supreme Commander Building, among others. As of April 7, 42 cases were listed in the red tag category (32 in Hualien, 2 in Taipei, 4 in Taoyuan, and 4 in New Taipei), and 70 cases in the yellow tag category (35 in Hualien, 13 in Taipei, 14 in Taoyuan, 7 in New Taipei, and 1 in Keelung). Overall, the actual disaster situation closely aligns with the estimated results of Scenario 1.

Table 3-1 Estimated Building Damage Results (Scenario 1)

County/City	Low-rise buildings (1–3 floors)	Mid-rise buildings (4–7 floors)	High-rise buildings (8–18 floors)	Total number of buildings
Hualien County	38	17	1	55
Yilan County	17	6	0	23

Table 3-2 Estimated Building Damage Results (Scenario 2)

County/City	Low-rise buildings (1–3 floors)	Mid-rise buildings (4–7 floors)	High-rise buildings (8–18 floors)	Total number of buildings
Hualien County	454	72	2	528
Yilan County	93	26	1	119
Taipei City	0	3	0	3

Table 3-3 Estimated Casualties Results (Scenario 1)

County/City	Severely injured and in critical condition	Immediate death
Hualien County	3	2
Yilan County	1	1

Table 3-4 Estimated Casualties Results (Scenario 2)

County/City	Severely injured and in critical condition	Immediate death
Hualien County	48	36
Yilan County	11	8
Taipei City	1	0

4. Building Damage Assessment

The seismic damage investigation reveals that existing buildings completed before the 921 earthquake in 1999 often exhibit poor structural system configurations. For instance, due to the need for commercial spaces, these buildings frequently feature high ceilings and void spaces on lower floors, leading to what is colloquially termed as "soft-story” buildings. Additionally, improper positioning of main reinforcement joints, excessive spacing between stirrups, and stirrup hooks bent at 90° during construction are common issues. These issues often result in inadequate strength and deformation capacity of the building's column components. Furthermore, many buildings have numerous partition walls, with sudden reductions in wall quantity on the ground floor, causing seismic forces to concentrate on lower floors. These ground-level "soft-story" buildings are primarily characterized by their open spaces on lower floors for public use, resulting in fewer structural and non-structural walls. Coupled with traditional arcade-style designs, this further weakens the seismic resistance of the ground level.

The acceleration response spectra obtained from the HWA019 station in Hualien City, as depicted in Figure 4-1, were compared with the design response spectra prescribed by the current seismic design regulations in Taiwan. It was found that both the short-period (0.3-sec) and long-period (1.0-sec) spectral accelerations from the station exceeded the maximum considered earthquake spectral acceleration values specified in the existing seismic design regulations.

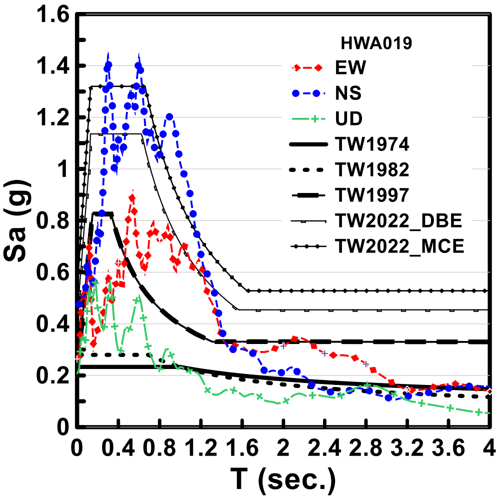

Figure 4-1 Acceleration Response Spectrum of Station HWA019

Figure 4-2 Collapse of Tianwangxing Building in Hualien

Figure 4-3 Severe Damage to the Ground Floor of a 6-Story Residential Building in Hualien

The damaged buildings depicted in Figures 4-2 and 4-3 are characterized by their triangular window arcade-style structures. These buildings exhibit irregularities in their structural plans and possess soft-story characteristics, making them susceptible to collapse or severe damage at lower levels during this earthquake.

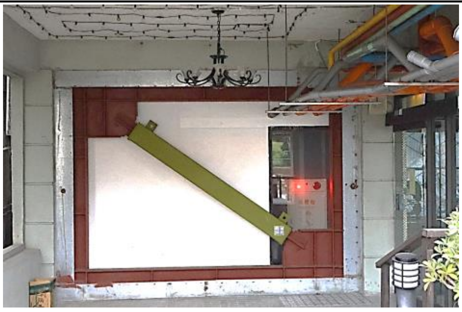

Figure 4-4 Hotel Structure Reinforced with BRB in Hualien City

Figure 4-5 Office Building Reinforced with SBRB in Hualien City

As depicted in Figures 4-4 and 4-5, both structures implemented buckling-restrained braces (BRBs) for strengthening at their lower levels. During this earthquake, these two buildings showed no significant damage, indicating the effectiveness of the strengthening measures implemented.

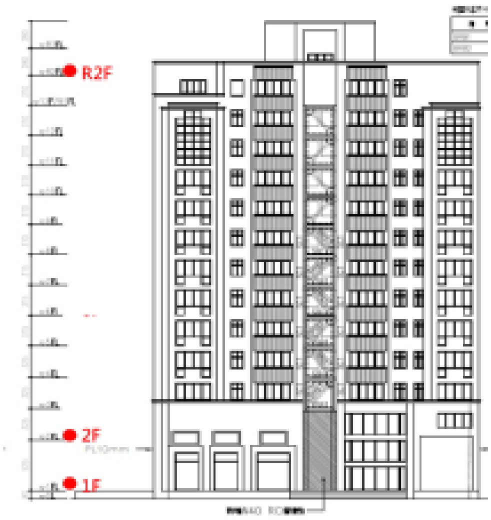

Figure 4-6 Elevation Plan of Reinforced Building A00600 in Taipei City

In addition, in a case study of a building in Taipei City that has undergone seismic strengthening measures (as shown in Figure 4-6), the building's ground floor was reinforced with reinforced concrete walls, while steel frame diagonal braces were used for reinforcement on other floors. Accelerometers were installed on the ground-floor base, the second-floor slab, and the roof slab for structural monitoring. The monitoring results from this earthquake are as follows:

• Seismic Intensity: 5-Weak

• Structural Damage Severity: Light

• Maximum Acceleration on 1st-floor slab: 86.2 gal

• Maximum Acceleration on 2nd-floor slab: 90.0 gal

• Maximum Acceleration on roof slab: 266 gal

• Displacement Ratio (1st floor): 0.295% (Safety threshold: 0.250%)

• Displacement Ratio (2nd floor and above): 0.146% (Safety threshold: 0.250%)

The building exhibited only minor structural damage during this earthquake, indicating the effectiveness of its seismic strengthening measures, demonstrating good seismic performance.

5. Geotechnical Disaster Survey

The seismic impacts in the Hualien region mainly resulted in landslides, rockfalls, and slope failures in mountainous areas. Significant damage to geotechnical structures occurred primarily in the Hualien Port area. Considering the urgent need for emergency response due to road collapses and the mountainous terrain, our center focused solely on conducting damage assessments in the Hualien Port area. We collaborated with National Taiwan University, National Yang Ming Chiao Tung University, National Chung Hsing University, National Cheng Kung University, National Sun Yat-sen University, and others to plan field visits. Hualien Port is situated northeast of Hualien City, bordering the Pacific Ocean to the east and backed by the Meilun Mountain to the west. Since its establishment as an international port in 1963, expansion projects were completed in 1973, 1977, and 1990. The port currently comprises a total of 25 piers, including 16 in the inner port area with water depths ranging 6.5–10.5 m, capable of accommodating vessels of 4,000–12,000 metric tons. The outer port area consists of 9 piers with water depths ranging 12–16.5 m, capable of accommodating vessels of 30,000 to 60,000 metric tons. This area was severely affected by the earthquake, making it the most heavily impacted region. The main focus of our assessment was on the areas around piers 25, 24, and 23, as illustrated in Figure 5-1.

Figure 5-1 Schematic Diagram of Hualien Port Pier Area

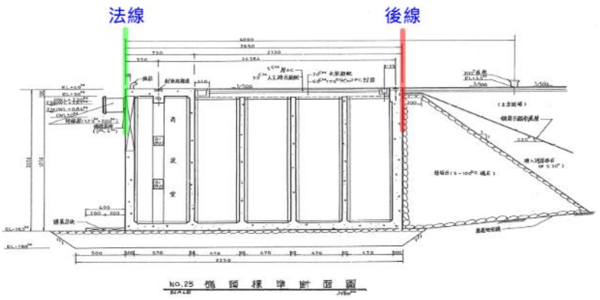

Figure 5-2 Cross-sectional Design of Pier 25 at Hualien Port (Source: Hualien Port Authority)

Hualien Port's pier 25 is a gravity caisson wharf with a structure width of 28.5 m. It features a wave-dissipating chamber structure at the front edge and is designed with a water depth of 16.5 m and a length of 332 m, primarily for general cargo handling. The standard cross-section design of pier 25 is illustrated in Figure 5-2. During this earthquake, pier 25 experienced more severe damage compared to neighboring piers 23 and 24. Significant differential settlement occurred at the joint between pier 25 and its wharf apron, with surface settlement reaching 70 cm at the wharf apron, as shown in Figure 5-3. Similar phenomena were observed at piers 23 and 24. The differential settlement of piers and wharf apron in the Hualien Port area due to the earthquake is summarized in Table 5-1.

Figure 5-3 Damage to Pier 25 and Wharf Apron at Hualien Port

Table 5-1 Maximum Settlement of Hualien Port Piers

Pier Number	Maximum Settlement
#25	70 cm
#23~#24	50 cm
#19~#22*	50 cm
#17~#18*	12 cm

* Provided by Hualien Port Authority

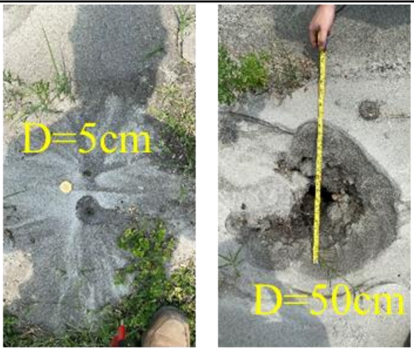

Figure 5-4 Sand vents in the Gravel Backfill Area of Pier 25 at Hualien Port

In addition, evident sand vents and cracks were found in the gravel backfill area behind the pier line. Observation indicated that the material ejected from the sand vents and surrounding cracks appeared as milky white sand with varying sizes of gravel, distinct from the surrounding soil, as shown in Figure 5-4. This phenomenon is attributed to the excessive pore water pressure generated by soil liquefaction. Apart from fine sand, larger gravel particles were also brought to the surface by the water pressure. Notably, there is significant variation in the diameter of the sand vents generated in the gravel backfill area. Among them, sand vents with diameters of up to 50 cm were measured to have depths exceeding 100 cm. This is a rare occurrence of sand vents resulting from soil liquefaction and can serve as a valuable reference for subsequent studies on soil liquefaction in gravel layers.

6. Non-structural Components and Systems

From April 13th to 14th, NCREE personnel visited Hualien City and Shoufeng Township, Hualien County, to survey non-structural components and systems (NSCS) in critical facilities, *i.e.*, three hospitals and a university. The following is a brief introduction to the surveyed NSCS including architectural components (T-bar ceilings, and non-structural walls), mechanical and electrical equipment (cooling towers and water tanks, elevators, and air-conditioning equipment), and building contents (library shelves).

1. T-bar ceilings: T-bar ceilings suffered widespread and significant damage during this seismic event, which is attributable to inadequate grid strength and improper seismic installation. Fig. 6-1 depicts the ceiling damage inside a university library in Hualien County (left figure), and in multiple classrooms across the university campus, with instances of light fixtures and ceiling fans falling (right figure).

2. Non-structural walls: after the earthquake, damages to non-structural walls, including masonry walls and lightweight aggregate concrete (LWAC) walls, were investigated. In the fifth- and sixth-floor wards of a hospital in Hualien City, multiple instances of shear damage were observed on the masonry walls, which are oriented along the northwest to southeast direction (Fig. 6-2).

3. Cooling towers and water tanks: Damage to cooling towers made of fiber-reinforced plastic (FRP) was observed on the rooftops of buildings in two hospitals in Hualien City. In the case of one of the hospitals, the base of the cooling tower on the rooftop of a building was damaged and tilted, as shown in Fig. 6-3. During the earthquake, the metal water tower on the rooftop of a hospital building in Hualien City was damaged. In addition to the damage to the water tower itself, its supporting base was also distorted and deformed under the overall inertial force and hydrodynamic pressure exerted by the water tower, as shown in Fig. 6-4 (left). In addition, another hospital building in Hualien City suffered damage to a FRP water tank located on the basement floor. This water tank is composed of FRP panels in vertical and horizontal steel frames. Because of the lack of connection at the joints of the vertical steel frames, the inertia force resulting in tearing of the FRP panels and water leakage, as shown in Fig. 6-4 (right).

4. Elevators: Three of the four elevators in a medium-sized hospital in Shoufeng Township could not be used immediately after the earthquake. One elevator was rendered unusable because of the significant displacement of the overhead hoist machine located in the elevator machine room on the roof floor, causing the associated cable to detach (Fig. 6-5, left). The other two elevators were rendered inoperable because parts of the mass blocks fell out of their counterweights. The blocks then damaged the elevator cars below (Fig. 6-5, right).

5. Air-conditioning equipment: Damage caused by air-conditioning equipment was observed in three hospitals across Hualien County and City. In a hospital in Hualien City, damage to the air-conditioning equipment on the catwalk level included ruptured and detached chilled-water pipes from the air-conditioning unit, broken suspension rods of the ventilation fan, and damage to the ductwork around the ventilation fan, as shown in Fig. 6-6.

8. Library shelves: A six-floor SRC (Steel-reinforced concrete) library was part of a university in Hualien City. Without anchorages, these free-standing bookshelves underwent sliding, rocking, and overturning during the earthquake, leading to books falling off and shelves being deformed, as shown in Fig. 6-7. Approximately 90% of the books fell from the bookshelves. The majority of earthquake damage occurred on the second to the sixth floors.

Fig. 6-1 Extensive ceiling collapse occurred inside the library (left) and light fixtures and ceiling fans fell in the classrooms (right) (PGA: 321 Gal).

Fig. 6-2 Both sides of the masonry walls were cracked (PGA: 418 Gal).

Fig. 6-3 The base of the FRP cooling tower was damaged and tilted (PGA: 395 Gal).

Fig. 6-4 The water tower and supporting base were deformed (left figure, PGA: 418 Gal), and the panels of the FRP water tank ruptured, resulting in water loss (right figure, PGA: 395 Gal).

Fig. 6-5 The hoist machine of one elevator was displaced (left) and mass blocks fell out of the counterweight of the other elevator (right) (PGA: 366 Gal).

Fig. 6-6 The chilled-water pipe rupture and detachment from the air conditioning unit (left), broken suspension rod of the ventilation fan (middle), and damage to the ductwork around the ventilation fan (right) (PGA: 395 Gal).

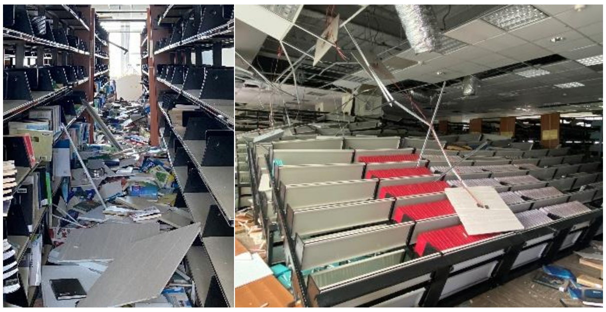

Fig. 6-7 Books falling and bookshelves overturing (PGA: 321 Gal).

7. Structural Responses of Seismically Isolated Structures

The regions most affected by the April 3, 2024, Hualien earthquake were the eastern and northwestern areas of Taiwan. It was the largest earthquake experienced by many existing base-isolated buildings in these areas. After the earthquake, the Chinese Society of Seismic Isolation, in collaboration with the National Center for Research on Earthquake Engineering, visited the Hualien and Greater Taipei areas to inspect and examine hospitals, schools, government buildings, and multiple private residences using seismic isolation technology. The findings from these inspections can be summarized as follows:

1. None of the seismically isolated buildings exhibited any structural damage, and the isolators and dampers within the isolation systems also showed no signs of damage.

2. In the superstructures of the seismically isolated buildings, there was almost no damage to non-structural components or indoor items.

3. Components spanning the isolation gaps (such as movable cover plates for walkways, driveways, and suspended elevators, and architectural finishes, etc.) experienced compression, deformation, or collision damage due to inadequate gap allowances.

4. The fireproof mortar or sealants used on the base-isolation system's fire covers were damaged or extruded due to movement of isolation systems.

5. Insufficient vertical space for isolation movement led to local damage to non-structural material.

6. Waterproofing materials in the gaps between the superstructure and substructure were squeezed, flipped, or deformed due to the motion of the isolation system.

7. Some structures were equipped with instrumentation systems, but, owing to inadequate maintenance, electrical systems failed and sensors lost functionality.

NTU Civil Engineering Research Building

The NTU Civil Engineering Research Building (Figure 7-1(a)) is a precast reinforced-concrete mid-story seismically isolated structure, comprising one basement, nine above-ground levels, and two penthouse levels. The isolation layer is situated on the second floor

(Figure 7-1(b)). The building includes laboratories, professors' research offices, administrative offices, student research rooms, and multipurpose classrooms. The base-isolation system (Figure 7-1(c)) consists of nineteen lead rubber bearings (LRB) with a diameter of 900 mm, along with two liquid viscous dampers (VD) in the longitudinal direction and four in the transverse direction. The dampers have a stroke of ±500 mm, a maximum force of 100 tons, and a non-linear index of 0.6.

After the April 3 earthquake event, an immediate inspection was conducted, confirming that the earthquake caused no damage to the structure or the isolation system. However, some minor non-structural damages occurred because of the movement of the isolation system, which can be easily restored and repaired. As shown in Figure 7-2(a), the movable cover plate for the suspended elevator below the isolation layer exhibited slight misalignment and compression deformation. The waterproof sealing strip between the superstructure and substructure was flipped, and its fasteners loosened (Figure 7-2(b)). The flexible fire-resistant material between the fireproof covers of the isolation units was damaged, deformed, or extruded as a result of deformation of the isolation units (Figure 7-2(c)).

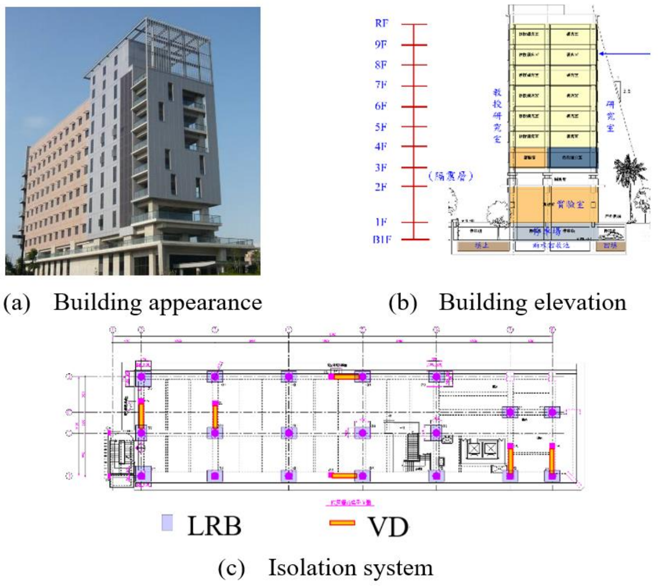

Fig. 7-1 The NTU Civil Engineering Research Building.

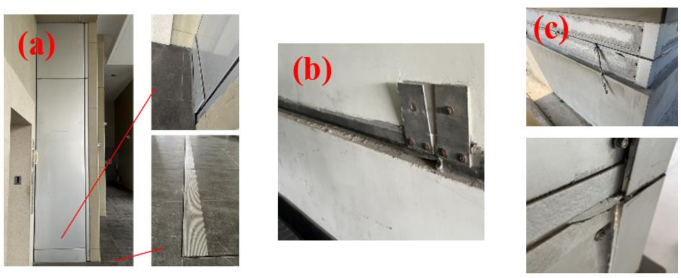

Fig. 7-2 Non-structural damages to the NTU Civil Engineering Research Building.

The structure is equipped with 27 accelerometers and four displacement transducers. The accelerometers are located on the basement floor, the second floor (below the isolation layer), the third floor (above the isolation layer), the sixth floor, and the roof, while the displacement transducers are installed in the isolation layer. The maximum displacements in the longitudinal and transverse directions were 21 mm and 16 mm, respectively (Figure 7-3). Summarizing the peak accelerations in the longitudinal and transverse directions for each floor (Table 7-1) reveals no significant dynamic amplification effect in the superstructure. The reduction efficiency in the long and short directions was 21% (= 100% − 79%) and 37% (= 100% − 63%), respectively.

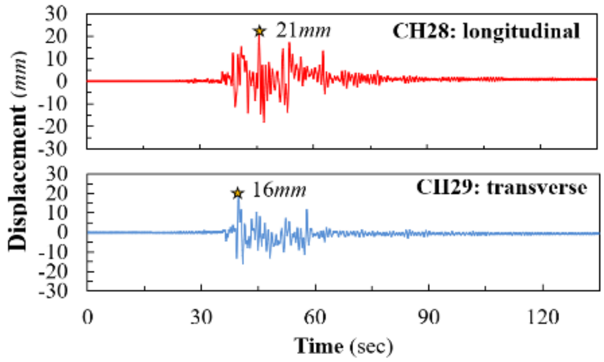

Fig. 7-3 Non-structural damages to the NTU Civil Engineering Research Building.

Table 7-1 Peak accelerations of each floor.

(unit: gal)

Floor	longitudinal	transverse
RF	62	78
6F	61	64
3F	77	60
2F	97	95
B1F	76	90
RF / 2F	64%	82%
6F / 2F	63%	67%
3F / 2F	79%	63%
2F / B1F	128%	106%

The HeXin Building

The Hualien TzuChi Medical Center stands as the premier medical facility in eastern Taiwan (Figure 7-4(a)). The HeXin Building within it primarily provides emergency, operating rooms, and general and intensive care wards. It is a steel-reinforced-concrete, seismically base-isolated building with eleven above-ground floors and one basement level. The isolation system is located beneath the first basement floor. The isolation system, which is designed to adjust the stiffness center according to the structural mass center, consists of 74 lead rubber bearings with diameters ranging from 800 mm to 1200 mm, along with fourteen plane sliding bearings without additional dampers.

(a) Building appearance (b) Numerical model

Fig. 7-4 The HeXin Building of the Hualien TzuChi Medical Center.

An inspection conducted on April 13 revealed no structural damage to the Hexin Building, thanks to the function of the isolation system. However, some non-structural components suffered damage due to inadequate allowance for isolation movement (Figures 7-5(a)–(c)). In contrast, the Xieli Building, a traditional aseismic structure, experienced various structural and non-structural damages. This demonstrates that base-isolation design not only effectively reduces structural seismic response but also significantly lowers the risk of non-structural component and equipment damage.

The structure is equipped with 26 accelerometers and four displacement transducers, all of which were damaged in previous earthquakes. The accelerometers are installed at the foundation (below the isolation layer), the first basement floor (above the isolation layer), and the fourth, fifth, and roof floors. Each floor has longitudinal and transverse accelerometers installed at both the center and corners of each floor. As shown in Figure 7-6, the overlap between longitudinal and transverse records indicates that no torsion occurred in the structure. Moreover, after transmission through the isolation system, seismic excitation led to reduced acceleration and an increased oscillation period. According to the peak acceleration from each floor in Table 7-2, the reduction efficiency in the longitudinal direction was between 20% and 30%, while the transverse reduction was less pronounced but exhibited no signs of dynamic amplification.

(a) Parterre (b) Walkway (c) Driveway

Fig. 7-5 The HeXin Building's nonstructural damages.

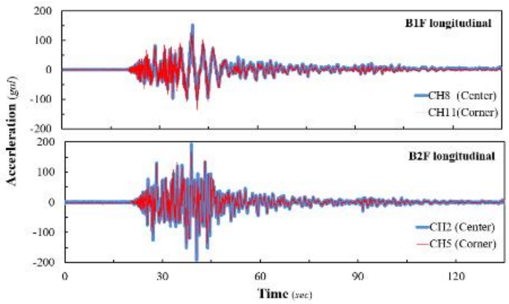

Fig. 7-6 Acceleration histories of the HeXin Building.

Table 7-2 Summary of maximum acceleration.

(unit: gal)

Floor	longitudinal	transverse
11F	152	290
5F	148	202
4F	135	198
B1F	152	200
B2F	194	209
11F / B2F	78%	139%
5F / B2F	76%	97%
4F / B2F	70%	95%
B1F / B2F	78%	96%

The acceleration history recorded at the foundation was used as input for numerical analysis (Figure 7-4(b)). Once the results aligned with the real responses (Figure 7-7(left)), the base-isolation displacement was estimated (Figure 7-7(right)), revealing maximum displacements of 27 cm and 45 cm in the longitudinal and transverse directions, respectively.

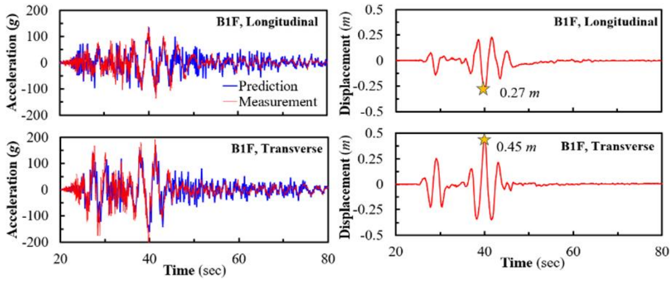

Fig. 7-7 (left) Comparison of real responses and predictions. (right) Predicted isolation displacement.

Summary

The April 3, 2024, Hualien earthquake caused significant structural responses in many seismically isolated buildings located in the eastern and northwestern areas of Taiwan. However, thanks to the functionality of isolation systems, buildings such as the HeXin Building in the Hualien TzuChi Medical Center, even when exposed to a strong near-fault earthquake with an intensity of −6, sustained no structural damage. Nonetheless, regarding the damage to non-structural components in seismically isolated buildings due to isolation displacement, two crucial issues arise: whether sufficient gaps have been allowed for isolation movement and whether building users can safely avoid hazards during base-isolation movement. These are critical questions that should be carefully addressed.

NCREE Earthquake Emergency Response Taskforce

Chung-Che Chou, Chiun-Lin Wu, Juin-Fu Chai
George C. Yao, Yu-Wen Chang, Jyun-Yan Huang
Chin-Hsun Yeh, Lee-Hui Huang, Yuan-Tao Weng
Tsung-Chih Chiou, Min-Lang Lin, Hsuan-Chih Yang
Kuan-Yu Chen, Fan-Ru Lin, Wei-Chung Chen
Wei-Hung Hsu, Bai-Yi Huang, Min-Chi Ko, Ya-Yu Hsiao
Chung-Han Yu, Shiang-Jung Wang, Cho-Yen Yang
Wang-Chuen Lin, Shen-Kai Peng, Yu-Fan Tseng
Che-Min Lin, Chi-Hao Lin

05/15/2024